ELSEVIER

Enhancements to the continuous wavelet transform for damping identifications on short signals

Miha Boltežar*, Janko Slavič

Faculty of Mechanical Engineering, University of Ljubljana, Aškerčeva 6, 1000 Ljubljana, Slovenia

Abstract

The edge-effect of the wavelet transform can present a serious limitation to the identification of damping. In an attempt to overcome the problem posed by the edge-effect, this paper presents three new methods that are incorporated into the definition of the continuous wavelet transform: the *reflected-window method*, the *equal-window-area method* and the *adaptive-wavelet-function method*. The effectiveness of these methods was tested on experimental data. It was found that with these methods the same rate of reliability could be achieved with a signal that was approximately three times shorter than the signal required by the classical CWT approach to damping identification.
© 2004 Elsevier Ltd. All rights reserved.

Keywords: Wavelet transform; Damping; Edge-effect

1. Introduction

The identification of damping in multi-degree-of-freedom systems is a well-known problem. A good overview of the different procedures for damping identification is given in the work of Staszewski [1]. The continuous wavelet transform (CWT) has proved to be very successful in the identification of damping [1–4], and has been shown to be highly resistant to noise [1]. In a recent study we showed a resistance of up to 0 dB signal-to-noise ratio [5].

Despite the good results obtained with the CWT, the edge-effect was found to be cumbersome for relatively short signals. This edge-effect has been studied in a variety of research areas, for example, weather analysis [6,7], geodesy [8], mechanics [1,2]. The cone-of-influence [6,9], also known as the radius-of-trust (time-width of the edge-effect), was already qualitatively

---

*Corresponding author. Tel.: +386-1-4771-608; fax: +386-1-2518-567.

E-mail address: miha.boltezar@fs.uni-lj.si (M. Boltežar).

characterised [5,10]. Kijewski and Kareem [9] used a simple padding scheme to meliorate the edge-effect. Padding is one of the simplest methods of meliorating the edge-effect. There are also other methods for reducing the edge-effect: zero padding, value padding, decay padding, repeating the signal, reflecting the signal [11]. There are also more advanced methods, such as extrapolating with non-linear models [8].

Previous research on the edge-effect was based on modifying the signal; this paper takes a different direction: it uses CWT modifications to enhance the damping identification at the edges.

The paper is organised as follows: The second section gives some of the basics of damping identification with the continuous wavelet transform. The third and fourth sections discuss the edge-effect and the reduction of the edge-effect, respectively. In the fifth section the presented methods are used to analyse the damping on experimental data. The last section is devoted to the discussion and the conclusions.

2. The basics of damping identification with the continuous wavelet transform

In this section only a few basic definitions of the CWT and damping identification with the CWT will be given. For details about the wavelet transform the reader should refer to [12], and for details about damping identification the reader should refer to [1,2].

2.1. The continuous wavelet transform

The continuous wavelet transform (CWT) of the signal $f(t) \in L^2(\mathbf{R})$ is defined as:

$$Wf(u, s) = \int_{-\infty}^{+\infty} f(t)\psi^*_{u,s}(t)\,\mathrm{d}t, \tag{1}$$

where u and s are the translation and scale/dilation parameters, respectively [13], and $\psi^*_{u,s}(t)$ is the translated-and-scaled complex conjugate of the basic/mother wavelet function $\psi(t) \in L^2(\mathbf{R})$. The wavelet function is a normalised function (i.e. the norm is equal to 1) with an average value of zero [12,14].

In this study the Gabor wavelet function [12] was used:

$$\psi(t, \sigma, \eta) = w(t, \sigma)\mathrm{e}^{i\eta t} = \underbrace{\frac{1}{\sqrt[4]{\pi\,\sigma^2}}\,\mathrm{e}^{-(t^2/2\sigma^2)}}_{\text{Gaussian window}}\,\mathrm{e}^{i\eta t}. \tag{2}$$

The scaled-and-translated wavelet function is:

$$\psi_{u,s}(t) = \frac{1}{\sqrt{s}}\psi\left(\frac{t - u}{s}\right). \tag{3}$$

Some properties of the Gabor wavelet function are shown in Table 1. In the following sections we will give some attention to the frequency variance $\sigma^2_{\omega_{u,s}}$ and to the time variance $\sigma^2_{t_{u,s}}$. The first defines the frequency spread of the CWT and is therefore important at identifying the damping of close modes that could interfere. The time spread, on the other hand, defines the width of the edge-effect in time.

Table 1
Properties of the Gabor wavelet function [10]

Time centre	$\bar{u}_{u,s}$	u
Frequency centre	$\bar{\omega}_{u,s}$	$\dfrac{\eta}{s}$
Time variance	$\sigma^2_{t_{u,s}}$	$\dfrac{\sigma^2 s^2}{2}$
Frequency variance	$\sigma^2_{\omega_{u,s}}$	$\dfrac{1}{2\sigma^2 s^2}$

2.2. Damping identification

For an asymptotic sinusoidal signal, like the response function of a damped system, the CWT can be approximated by a simple function [15]. Staszewski [1] and Ruzzene et al. [2] used the Morlet wavelet function, and as a consequence they used the CWT approximation as defined by Delprat et al. [16]. The approximation for the Gabor wavelet is [5]:

$$Wx(u,s) = \frac{1}{2} A(u)\hat{\psi}_{\text{Gabor}_{u,s}}(\varphi'(u), \sigma, \eta)e^{i\varphi(u)} + Er(A'(t), \varphi''(u)), \tag{4}$$

where $\hat{\psi}_{\text{Gabor}_{u,s}}(\omega, \sigma, \eta)$ is the Fourier transform of the translated-and-scaled Gabor wavelet function [10]. The approximation error $Er(A'(t), \varphi''(u))$ can be neglected if the derivative of the phase $\varphi'(u)$ is greater than the bandwidth of the translated-and-scaled Gabor wavelet function $\Delta\omega$ [12].

If there is a need to analyse multi-degree-of-freedom systems, then the CWT of any two components i and j of a multi-component signal should not interfere. Therefore, the maximum of the bandwidths $\Delta\omega(s_i)$ and $\Delta\omega(s_j)$ should be smaller than the frequency difference of i and j [12]:

$$(\varphi'_i(u) - \varphi'_j(u)) \geqslant \max\{\Delta\omega(s_i), \Delta\omega(s_j)\} \tag{5}$$

In identifying the damping of mdof systems the assumption of proportional damping is made: $\mathbf{C} = \alpha\mathbf{M} + \beta\mathbf{K}$, where $\mathbf{C}$, $\mathbf{M}$ and $\mathbf{K}$ are the damping, the mass and the stiffness matrices, respectively. As a consequence of the proportionality the natural frequencies are uncoupled and can be studied independently [1].

For the free response of a damped signal [17]:

$$x(t) = A_0 e^{-\zeta\omega_0 t} \cos(\omega_d t + \phi), \tag{6}$$

where $\omega_d = \omega_0\sqrt{1 - \zeta^2}$ denotes the damped natural frequency. The damping identification is now straightforward. The CWT is calculated, and the *ridge* of the CWT is located, i.e. $s = s(u)$. And by using the approximation given by Eq. (4) and the approximation $\omega_d \approx \omega_0$, the following equation can be used to identify the damping [1,5]:

$$A(u) \approx \frac{2|Wx(u, s(u))|}{(4\pi\sigma^2 s(u)^2)^{1/4}}, \tag{7}$$

$$\ln(A(u)) \approx -\zeta\omega_d u + \ln A_0. \tag{8}$$

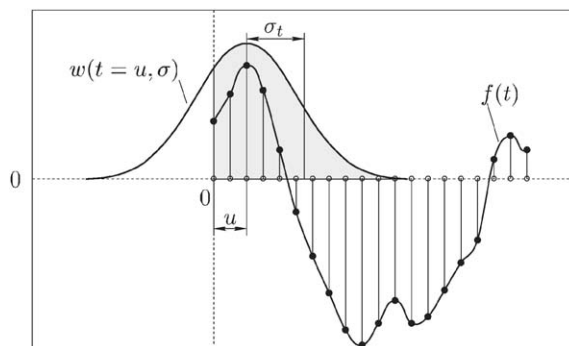The slope of $\ln(A(u))/\omega_d$ is simply the damping ratio.

Fig. 1. Window and the signal at the edge.

3. The edge-effect

The wavelet transform is usually computed by employing the convolution theorem. Because the convolution theorem covers some aspects of the edge-effect the wavelet transform in this study is bound to the integral in Eq. (1).

In order to demonstrate the edge-effect, Eq. (1) at some translation u is sketched in Fig. 1. It is clear that a major part of the window (shaded) is inside the signal; however, the part outside the signal makes the wavelet function non-symmetrical and the amplitude of the wavelet transform non-proportional to the amplitude of the wavelet transform without the edge-effect. This non-symmetry causes an error in the phase detection, and the non-proportionality causes an error in the amplitude detection.

From Fig. 1 it is clear that zero padding makes little sense; however, the effects on the convolution theorem of such padding are useful.

In the free response of a damped system the amplitudes at the beginning are high and at the end they are low. When using the circular-convolution theorem, care must be taken because the influence of the high amplitudes at the beginning results in low amplitudes at the end of the signal. The effect of circular convolution can be seen on the scalogram of Fig. 5, which is the only figure made using the convolution theorem in this paper.

The range of the edge-effect is described by the radius of trust [10]:

$$R(k, s, \sigma) = k\sigma_{t_{u,s}} = k\frac{\sigma s}{2}, \tag{9}$$

where k defines the multiple of the time spread. In signals with a relatively low variation of the amplitude a choice of $k = 3$–4 would be appropriate, but for a fast-changing (e.g. a highly damped) signal a higher value for k should be used. In this study $k = 6$ will be used.

4. Reduction of the edge-effect

4.1. The reflected-window (RFW) method

This method tries to improve the symmetry of the non-symmetrical window on the edge. The result is similar to the signal reflection, but in this case the window of the wavelet function is

reflected (Fig. 2). The advantage, apart the signal reflection, is the continuity of the phase, which is also shown in the amplitude detection.

The definition of the modified continuous wavelet transform is:

$$W_{\mathrm{RFW}}f(u,s) = \int_{-\infty}^{+\infty} f(t)\psi^*_{\mathrm{RFW}_{u,s}}(t)\,\mathrm{d}t, \tag{10}$$

where $\psi_{\mathrm{RFW}_{u,s}}$ is the modified Gabor wavelet function:

$$\psi_{\mathrm{RFW}_{u,s}}(t,\sigma,\eta) = \frac{1}{\sqrt{s}}\frac{1}{(\pi\sigma^2)^{1/4}}\left(\mathrm{e}^{-((t-u)/\sqrt{2}s\sigma)^2} + \mathrm{e}^{-((t+u)/\sqrt{2}s\sigma)^2} + \mathrm{e}^{-((t-(2T-u))/\sqrt{2}s\sigma)^2}\right)\mathrm{e}^{i\eta(t-u)/s}, \tag{11}$$

where T is the length of the signal.

4.2. The equal-window-area (EWA) method

With this method there is an attempt to keep the proportionality of the absolute value of the wavelet transform. On the edge, a part of the window is outside the signal (Fig. 3), therefore the value of the wavelet transform is increased by an amount equal to the fraction of the whole window area divided by the window area inside the signal.

At the beginning of the signal the part of the window inside the signal is:

$$P_0(u,s,\sigma) = \frac{\int_0^{+\infty} |\psi_{\mathrm{Gabor}_{u,s}}(t,\sigma,\eta)|\,\mathrm{d}t}{\int_{-\infty}^{+\infty} |\psi_{\mathrm{Gabor}_{u,s}}(t,\sigma,\eta)|\,\mathrm{d}t} = \frac{1 + \mathrm{Erf}\left(u/\sqrt{2}s\sigma\right)}{2} \tag{12}$$

and at the end of the signal (time T):

$$P_T(u,s,\sigma) = \frac{\int_{-\infty}^{+T} |\psi_{\mathrm{Gabor}_{u,s}}(t,\sigma,\eta)|\,\mathrm{d}t}{\int_{-\infty}^{+\infty} |\psi_{\mathrm{Gabor}_{u,s}}(t,\sigma,\eta)|\,\mathrm{d}t} = \frac{1 + \mathrm{Erf}\left((T-u)/\sqrt{2}s\sigma\right)}{2} \tag{13}$$

The definition of the modified continuous wavelet transform is:

$$W_{\mathrm{EWA}}f(u,s) = P_0(u,s,\sigma)^{-1}P_T(u,s,\sigma)^{-1}\int_{-\infty}^{+\infty} f(t)\psi^*_{u,s}(t)\,\mathrm{d}t \tag{14}$$
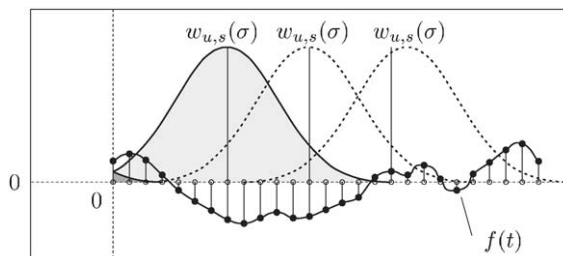

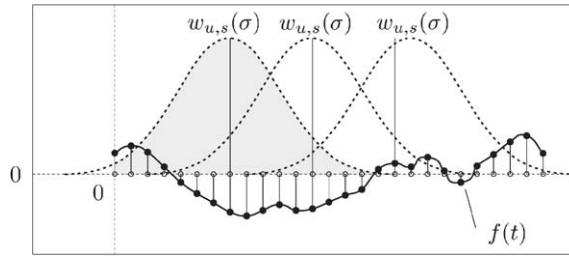
Fig. 2. Scheme of the reflected-window method.

Fig. 3. Scheme of the equal-window-area method.

4.3. The adaptive-wavelet-function (AWF) method

With the help of the parameter σ of the Gabor wavelet function it is easy to set the desired time or frequency spread (Table 1). Because the frequency spread changes, one should use this method with care, especially when identifying the damping of multi-degree-of-freedom systems, Eq. (5). For details about identifying damping at close modes, please refer to [5].

As already mentioned, it is necessary to choose a parameter σ that gives the desired time/ frequency spread. Then the parameter k of the radius of trust should be set. The radius of trust defines the range where the edge-effect should be treated. The idea of the AWF method is to adapt (at the edge) the time spread of the wavelet function to the defined radius of trust. In the middle of the signal the CWT is calculated with Eq. (1), but on the edge, instead of the chosen parameter σ, the parameter σ_R is used, see Eq. (17), as shown in Fig. 4.

To make the wavelet transform comparable for different parameters σ it has to be normalised. The definition of the modified continuous wavelet transform is:

$$W_{\mathrm{AWF}}f(u,s) = \begin{cases} & u < R(k,s,\sigma) \\ \sqrt{\dfrac{\sigma}{\sigma_R(k,u,s)}} \int_{-\infty}^{+\infty} f(t)\psi_{\mathrm{AWF}_{u,s}}^{*}(t)\,\mathrm{d}t, & \text{or} \\ & (T-u) < R(k,s,\sigma) \\ \int_{-\infty}^{+\infty} f(t)\psi_{u,s}^{*}(t)\,\mathrm{d}t & \text{elsewhere,} \end{cases} \tag{15}$$

where

$$\psi_{\mathrm{AWF}_{u,s}}(t,\sigma,\eta) = \frac{1}{\sqrt{s}} \frac{1}{(\pi\,\sigma_R^2(k,u,s))^{1/4}} \, \mathrm{e}^{-\left((t-u)/\sqrt{2}s\sigma_R(k,u,s)\right)^2} \mathrm{e}^{i\eta(t-u)/s}, \tag{16}$$

and

$$\sigma_R(k,u,s) = \begin{cases} \dfrac{2u}{ks}, & u < R(k,s,\sigma) \\ \dfrac{2(T-u)}{ks}, & (T-u) < R(k,s,\sigma) \end{cases} \tag{17}$$

Eq. (17) is derived from the radius-of-trust defined by Eq. (9).

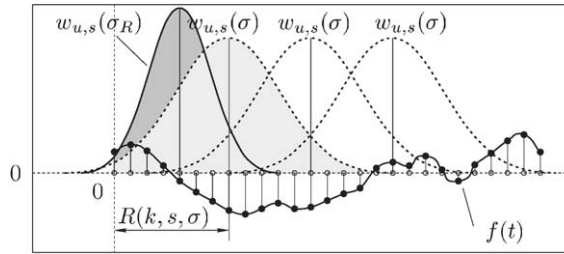Fig. 4. Scheme of the adaptive-wavelet-function method.

When u goes to 0 the time spread σ_R goes to zero, and consequently the frequency spread goes to infinity. Therefore, a minimum parameter $\sigma_{\min}$ that still provides an acceptable frequency spread has to be defined. If $\sigma_R < \sigma_{\min}$ then $\sigma_{\min}$ is used instead of σ_R.

As was shown in our recent studies [5,18], the use of a relatively small parameter σ leads to a frequency shift $\Delta\omega$ of the CWT amplitude:

$$\Delta\omega(s, \sigma, \eta) = \frac{\eta - \sqrt{2/\sigma^2 + \eta^2}}{2s}. \tag{18}$$

If the maximum allowed frequency shift is defined, then Eq. (18) can also be used to define $\sigma_{\min}$.

5. Experiment

The free response of a steel beam [5] with 15×30 mm^2 cross-section and 500 mm length is shown in Fig. 5.

The presented algorithms will be used to identify the hysteretic damping factor of the sixth natural frequency. Since the conventionally used symbol for the hysteretic damping factor η already denotes the frequency modulation of the wavelet transform the symbol $\acute{\eta}$ is used for the hysteretic damping factor.

The presented damping identification was carried out in terms of viscous damping, so we have to use the equivalent viscosity of hysteretic damping [19]:

$$\zeta = \frac{\acute{\eta}}{2}. \tag{19}$$

The parameters of the CWT were $\eta = 411\,775$ Hz and $\sigma_{1\text{ Hz}} = 10$. In the case of the truncated Morlet wavelet function [11] with central frequency $f_0 = 62.3$ Hz, similar effects would be achieved. These parameters are chosen to ensure a high noise resistance and to limit the frequency-shift error at 5592 Hz to less than 1 Hz [5].

As this paper focuses on short signals, the minimum time needed to get a relevant damping identification was searched for. The minimum time needed is approximately 2.5 times the width of the radius-of-trust R. The width of the useful signal is then $0.5 \times R$. In the case of the sixth natural frequency, $f_6 = 5592$ Hz, by using the parameter $k = 6$, the radius-of-trust is $R = 5.4$ ms, Eq. (9). Note: $R = 5.4$ ms at 5592 Hz represents approximately 30 periods of oscillation.

Figs. 6 and 7 show classical damping identification with the CWT and classical damping identification with the CWT using signal reflection, respectively. As noted in Fig. 6, in the case of the classical/unmodified CWT the damping identification was made on a width of $0.5R = 2.7$ ms (approx. 15 periods of oscillations), which is not affected by the edge.

Figs. 8–10 show damping identification with the CWT using the three proposed methods. For the adaptable-window method an additional parameter was used: $\sigma_{1\ Hz\ Min} = 1.5$.

Because the proposed methods reduce the edge-effect a broader time-width was used to identify the damping. From the $2.5 \times R = 13.5$-ms-long signal (75 oscillations), the useful part was 11.6 ms instead of 2.7 ms.

As can be seen from Table 2, the classical CWT and the classical CWT with signal reflection differ by more than 50% from the proposed methods. From Fig. 11 it is clear that the classical CWT method converges to $\acute{\eta} \approx 1480 \times 10^{-6}$ as the time-width of the signal enlarges. At a width of approximately 7 times the radius-of-trust ($7 \times R \approx 38$ ms), a similar level of confidence was reached as when using the RFW, EWA or AWF methods. With the proposed methods instead of a 38-ms-long signal a shorter signal can be used: $2.5 \times R \approx 13.5$ ms.
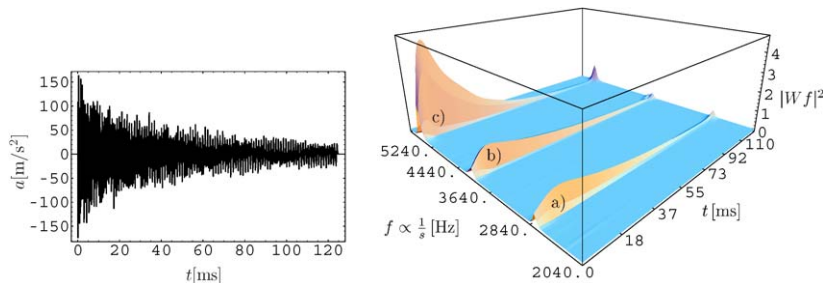

Fig. 5. Left: response of a free–free beam (125 ms); right: scalogram of (a) 4th, (b) 5th and (c) 6th natural frequency.
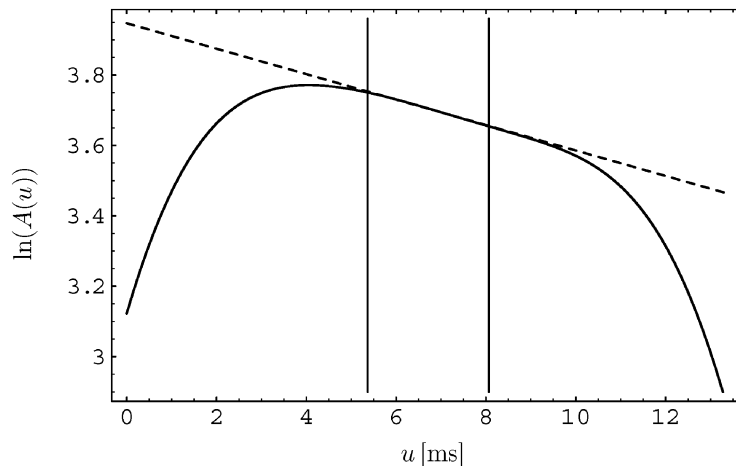

Fig. 6. $\ln(A(u))$ using the unmodified CWT definition. (- - -) linear approximation of $\ln(A(u))$ between vertical lines.
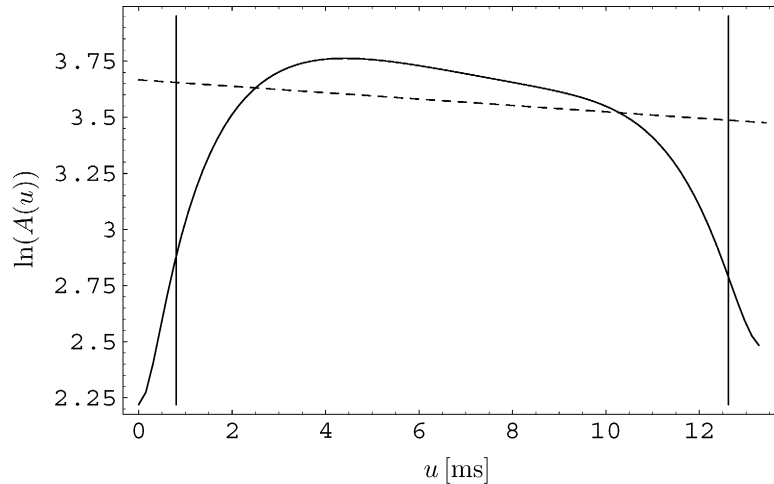
Fig. 7. $\ln(A(u))$ using the unmodified CWT definition and signal reflection. (- - -) linear approximation of $\ln(A(u))$ between vertical lines.
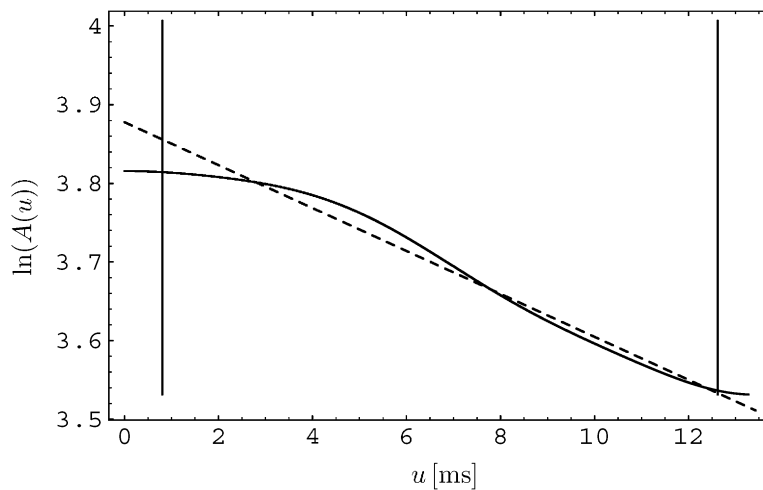

Fig. 8. $\ln(A(u))$ using the reflected-window method, Eq. (10). (- - -) linear approximation of $\ln(A(u))$ between vertical lines.

If we were to analyse similar damping of other natural frequencies the minimum time needed to make a reliable estimation would be the time that corresponds to approximately 75 periods of oscillation.

6. Discussion and conclusions

To identify the damping on short signals this paper introduces three modifications of the continuous wavelet transform in order to reduce the edge-effect: the *reflected-window method*, the *equal-window-area method* and the *adaptive-wavelet-function method*.
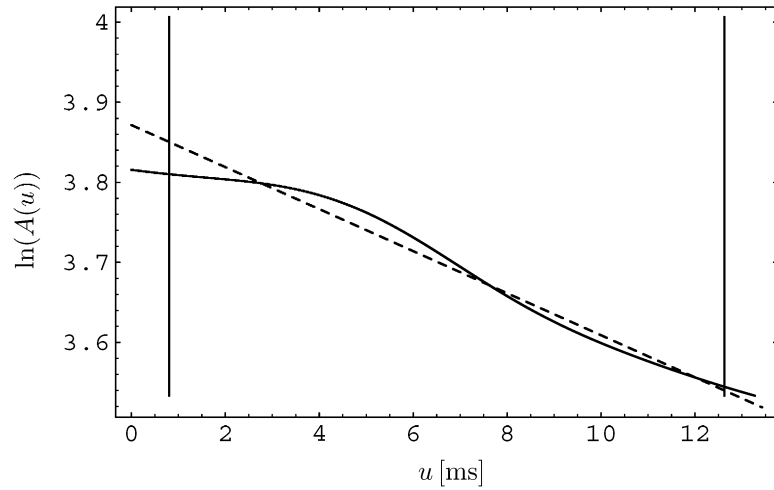
Fig. 9. $\ln(A(u))$ using the equal-window method, Eq. (14). (- - -) linear approximation of $\ln(A(u))$ between vertical lines.
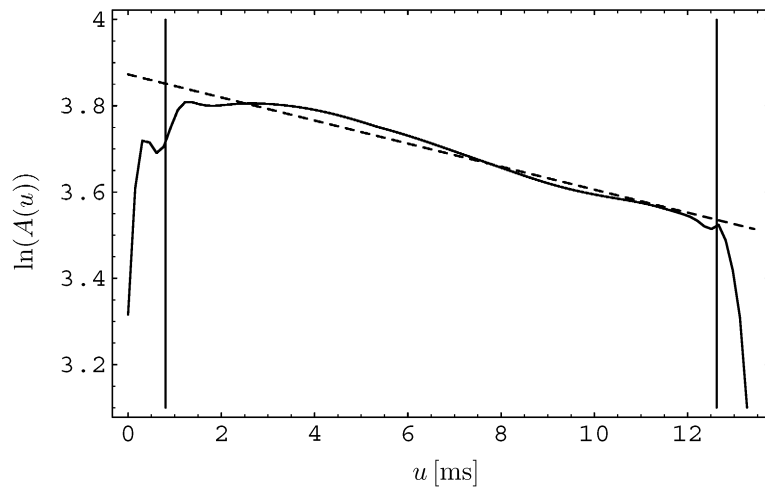

Fig. 10. $\ln(A(u))$ by using the adaptive-wavelet-function method, Eq. (15). (- - -) linear approximation of $\ln(A(u))$ between vertical lines.

Table 2
Identified hysteretic damping factor

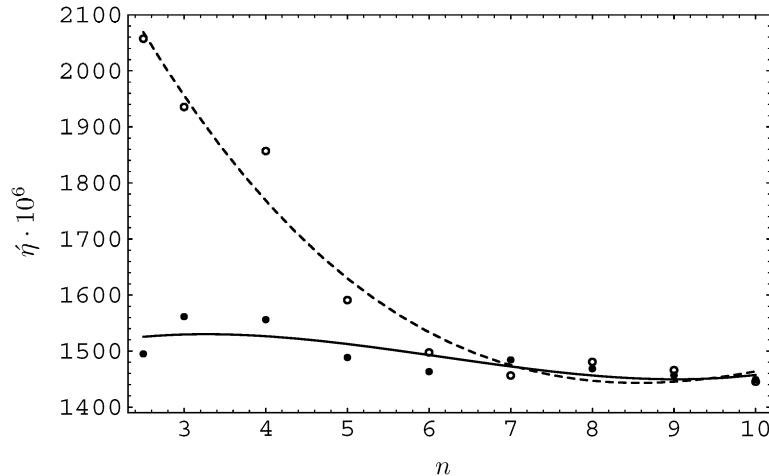| Method	$\acute{\eta} \times 10^6$
Classical CWT	2056
Classical CWT with sig. ref.	810
Reflected-window method	1554
Equal-window method	1495
Adaptable-window-function method	1519

Fig. 11. The convergence of the hysteretic damping factor by increasing the time-width of the signal. n is the number of radius-of-trust widths R. (- - -) and ($\circ$) represent the classical approach. (—) and ($\bullet$) represent the EWA method (the RFW and AWF methods give similar results).

In contrast to other researchers, the problem of the edge-effect has been solved here by modifying the wavelet transform, instead of trying to extend the signal [6–10].

The experimental data analysis showed that the proposed modifications to the continuous wavelet transform can be used to identify the damping during short signals. To ensure the same rate of reliability the signals were approximately three times shorter than the ones that were needed with the classical CWT approach to damping identification.

The classical reflected-time-series method does not ensure the continuity of the phase and its advantage on the edge is in doubt. This method does not give any improvements when identifying the damping with the CWT on short signals.

The adaptive-wavelet-function method gives promising results, but it should not be forgotten that the adaptive wavelet function varies the parameter σ, which changes the time–frequency spread of the Gabor mother wavelet. A high-frequency spread is not advisable with noisy signals [5] and with multi-component-signals that have close frequencies. The increasing frequency shift at the edge should also be taken care of.

The equal-window method and the reflected-window method both give relevant results, while the changes to the wavelet transform are easily implemented and do not need any additional parameters, as is the case with the AWF method.

In general we can conclude that the proposed methods give more reliable results at same time-length of the analysed signal.

References

[1] W. Staszewski, Identification of damping in MDOF systems using time-scale decomposition, Journal of Sound and Vibration 203 (2) (1997) 283–305.

[2] M. Ruzzene, A. Fasana, L. Garibaldi, B. Piombo, Natural frequencies and dampings identification using wavelet transform: application to real data, Mechanical Systems and Signal Processing 11 (2) (1997) 207–218.

[3] K. Demarchi, J.A. Craig, Comments on "natural frequencies and dampings identification using wavelet transform: application to real data", Mechanical Systems and Signal Processing 17 (2) (2003) 483–488.

[4] S. Hans, E. Ibraim, S. Pernot, C. Boutin, C.H. Lamarque, Damping identification in multi-degree-of-freedom systems via a wavelet-logarithmic decrement—Part 2: study of a civil engineering building, Journal of Sound and Vibration 235 (3) (2000) 375–403.

[5] J. Slavič, I. Simonovski, M. Boltežar, Damping identification using a continuous wavelet transform: application to real data, Journal of Sound and Vibration 262 (2003) 291–307.

[6] C. Torrence, G. Compo, A practical guide to wavelet analysis, Bulletin of the American Meteorological Society 79 (1) (1998) 61–78.

[7] S.D. Meyers, B.G. Kelly, J.J. O'Brien, An introduction to wavelet analysis in oceanography and meteorology: with application to the dispersion of Yanai waves, Monthly Weather Review 121 (1993) 2858–2866.

[8] D. Zheng, B. Chao, Y. Zhou, N. Yu, Improvement of edge effect of the wavelet time–frequency spectrum: application to the length-of-day series, Journal of Geodesy 256 (74) (2000) 249–254.

[9] T. Kijewski, A. Kareem, On the presence of end effects and their melioration in wavelet-based analysis, Journal of Sound and Vibration 256 (5) (2002) 980–988.

[10] I. Simonovski, M. Boltežar, The norms and variances of the Gabor, Morlet and general harmonic wavelet functions, Journal of Sound and Vibration 264 (3) (2003) 545–557.

[11] P. Addison, The Illustrated Wavelet Transform Handbook: Introductory Theory and Applications in Science, Engineering, Medicine and Finance, Institute of Physics, London, UK, 2002.

[12] S. Mallat, A Wavelet Tour of Signal Processing, 2nd Edition, Academic Press, New York, 1999.

[13] A. Grossman, J. Morlet, Decomposition of Hardy function into square integrable wavelets of constant shape, SIAM Journal of Mathematical Analysis and Applications 15 (4) (1984) 723–736.

[14] M. Boltežar, I. Simonovski, M. Furlan, Fault detection in DC electro motors using the continuous wavelet transform, Meccanica 38 (2) (2003) 251–264.

[15] P. Tchamitchian, B. Torresani, Ridge and skeleton extraction from the wavelet transform, in: M.B. Ruskai (Ed.), Wavelets and Their Applications, Jones and Bartlett Publishers International, Boston, London, 1992, pp. 123–151.

[16] N. Delprat, B. Escudie, P. Guillemain, R. Martinet, P. Tchamitchian, B. Torresani, Asymptotic wavelet and Gabor analysis: extraction of instantaneous frequencies, IEEE Transactions on Information Theorems 38, special issue on Wavelet and Multiresolution Analysis 2 (1992) 644–664.

[17] W. Thomson, Theory of Vibration with Applications, 4th Edition, Chapman & Hall, London, 1993.

[18] J. Slavič, M. Boltežar, Enhanced identification of damping using continuous wavelet transform, Journal of Mechanical Engineering 48 (11) (2002) 621–631.

[19] C. Beards, Structural Vibration: Analysis and Damping, Arnold, Paris, 1996.